

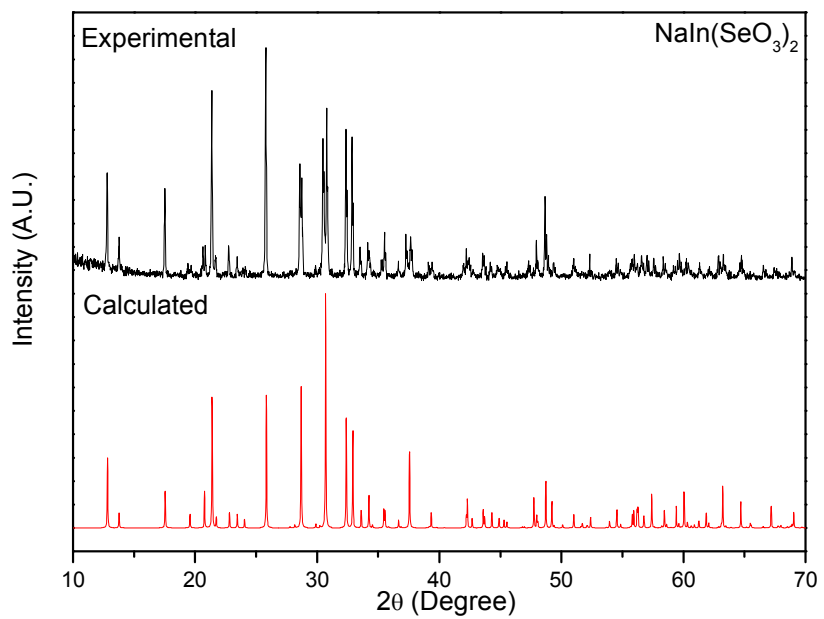
Cation Size Effect on the Framework Structures in a Series of New Alkali Metal Indium Selenites, AIn(SeO₃)₂ (A = Na, K, Rb, and Cs)

Dong Woo Lee, Saet Byeol Kim, and Kang Min Ok*

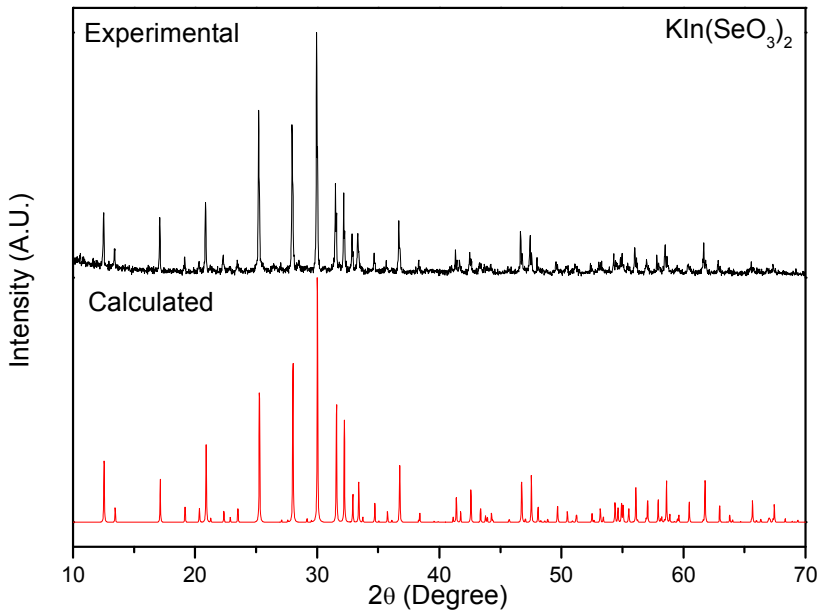
Department of Chemistry, Chung-Ang University, 221 Heukseok-dong, Dongjak-gu, Seoul 156-756, Republic
of Korea

- S1. Experimental and calculated powder X-ray diffraction patterns for NaIn(SeO₃)₂
- S2. Experimental and calculated powder X-ray diffraction patterns for KIn(SeO₃)₂
- S3. Experimental and calculated powder X-ray diffraction patterns for RbIn(SeO₃)₂**
- S4. Experimental and calculated powder X-ray diffraction patterns for CsIn(SeO₃)₂
- S5. Thermogravimetric analysis diagram for NaIn(SeO₃)₂
- S6. Thermogravimetric analysis diagram for KIn(SeO₃)₂
- S7. Thermogravimetric analysis diagram for RbIn(SeO₃)₂
- S8. Thermogravimetric analysis diagram for CsIn(SeO₃)₂
- S9. IR spectrum for NaIn(SeO₃)₂
- S10. IR spectrum for KIn(SeO₃)₂
- S11. IR spectrum for RbIn(SeO₃)₂
- S12. IR spectrum for CsIn(SeO₃)₂
- S13. ORTEP (50% probability ellipsoids) representations in KIn(SeO₃)₂ showing (a) the distorted InO₆ octahedron, (b) the asymmetric SeO₃ polyhedra, and (c) the KO₈ polyhedron.
- S14. ORTEP (50% probability ellipsoids) representations in RbIn(SeO₃)₂ showing (a) the distorted InO₆ octahedron, (b) the asymmetric SeO₃ polyhedra, and (c) the RbO₈ polyhedron.
- S15. ORTEP (50% probability ellipsoids) representations in CsIn(SeO₃)₂ exhibiting (a) the InO₆ octahedron, (b) the asymmetric SeO₃ polyhedra, and (c) the CsO₁₂ hexagonal prism.

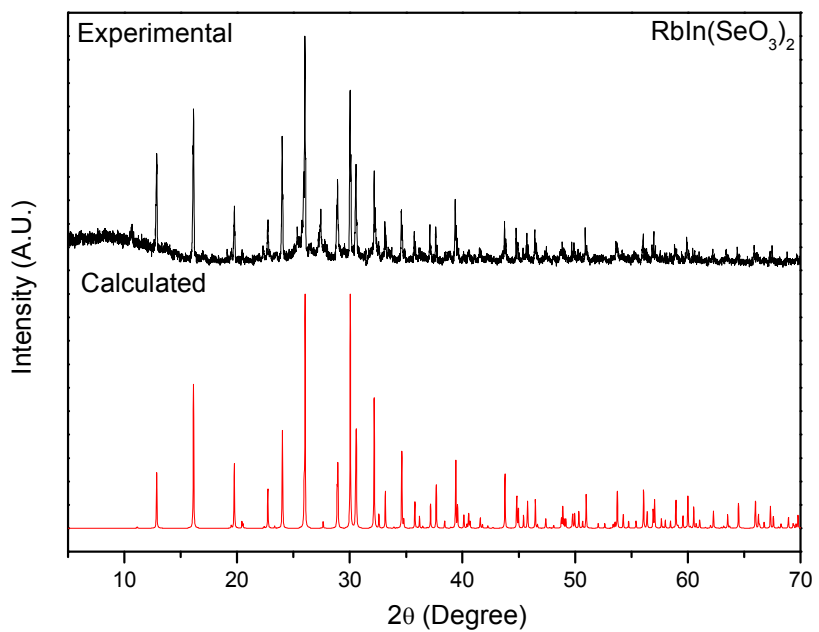
S1. Experimental and calculated powder X-ray diffraction patterns for $\text{NaIn}(\text{SeO}_3)_2$



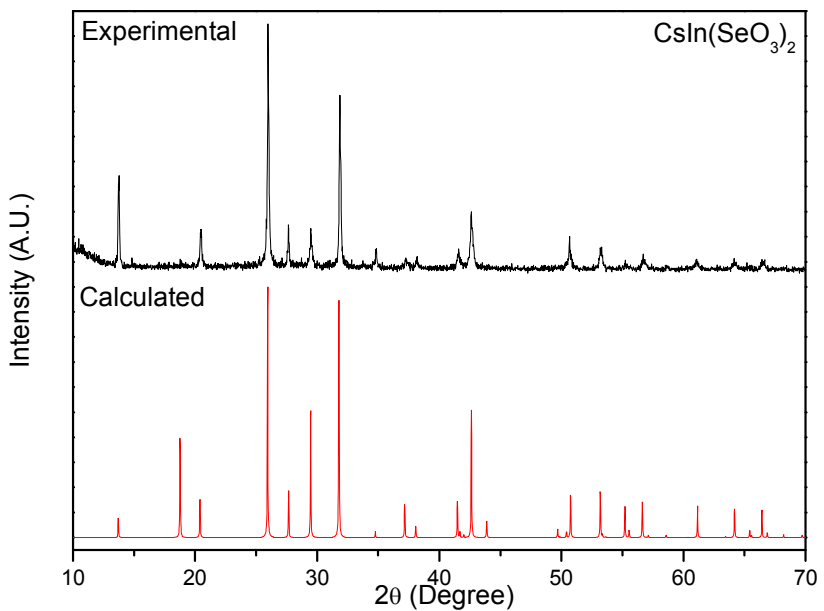
S2. Experimental and calculated powder X-ray diffraction patterns for $\text{KIn}(\text{SeO}_3)_2$



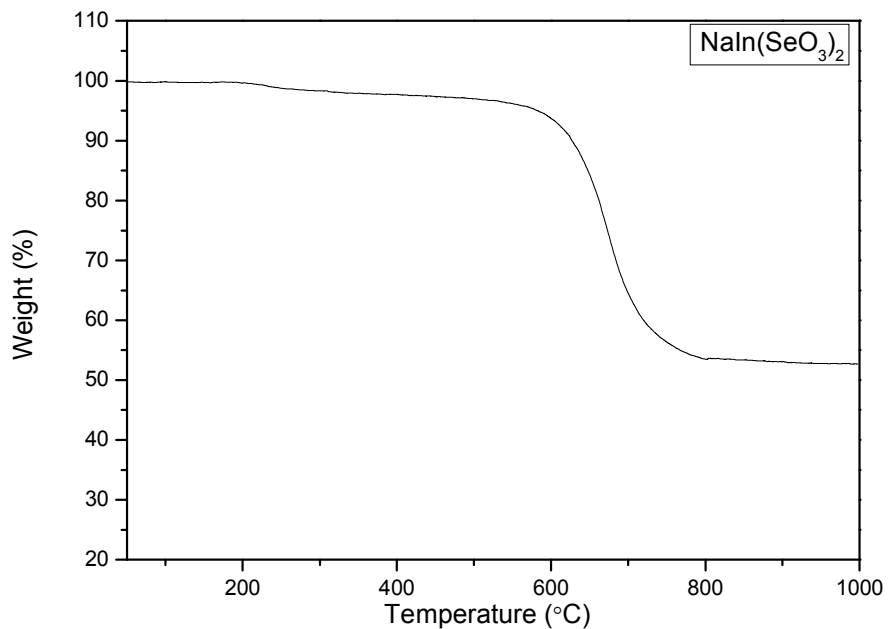
S3. Experimental and calculated powder X-ray diffraction patterns for $\text{RbIn}(\text{SeO}_3)_2$



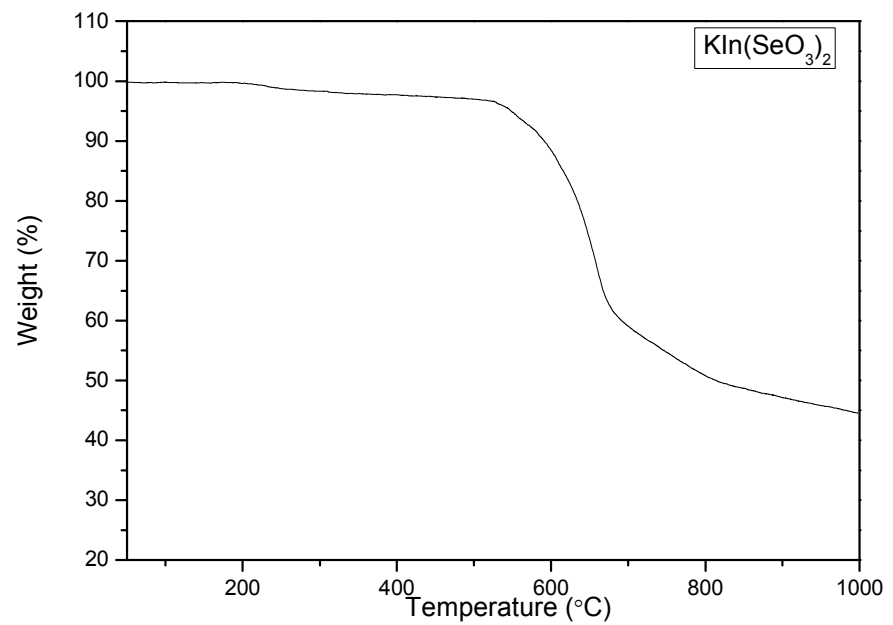
S4. Experimental and calculated powder X-ray diffraction patterns for $\text{CsIn}(\text{SeO}_3)_2$



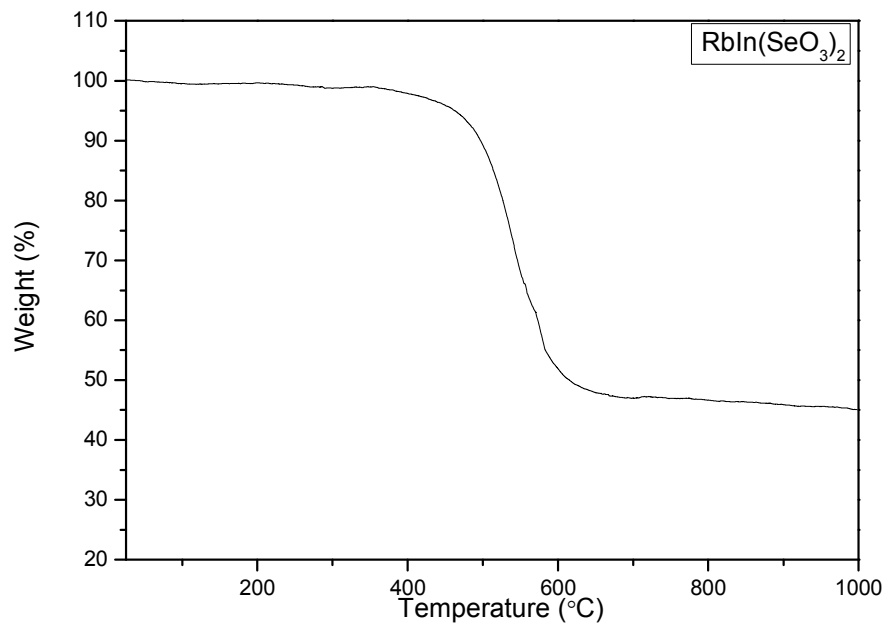
S5. Thermogravimetric analysis diagram for $\text{NaIn}(\text{SeO}_3)_2$



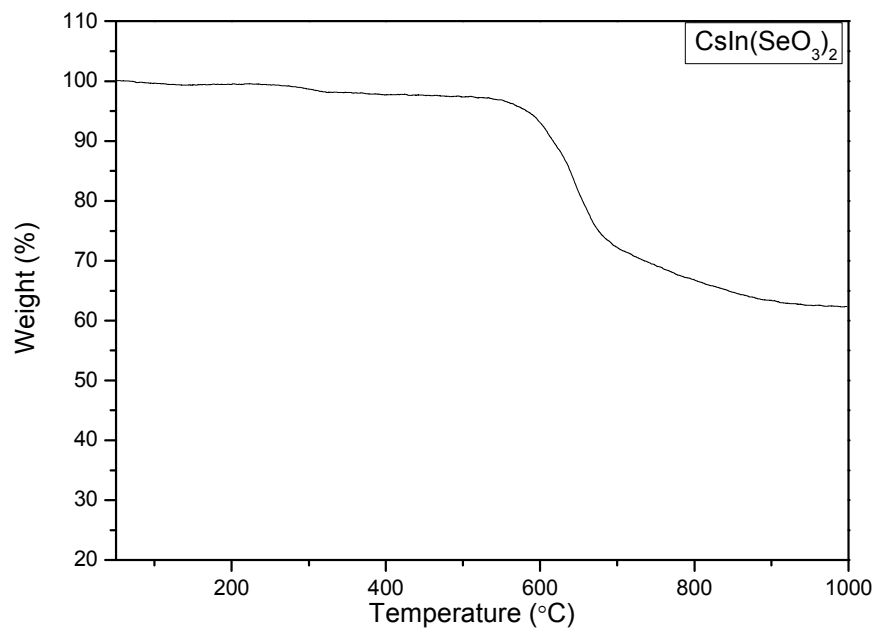
S6. Thermogravimetric analysis diagram for $\text{KIn}(\text{SeO}_3)_2$



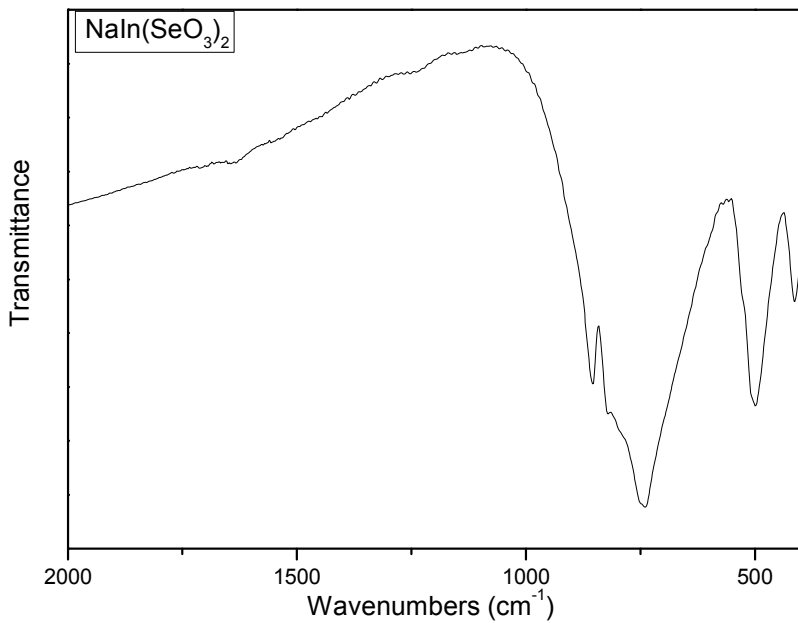
S7. Thermogravimetric analysis diagram for $\text{RbIn}(\text{SeO}_3)_2$



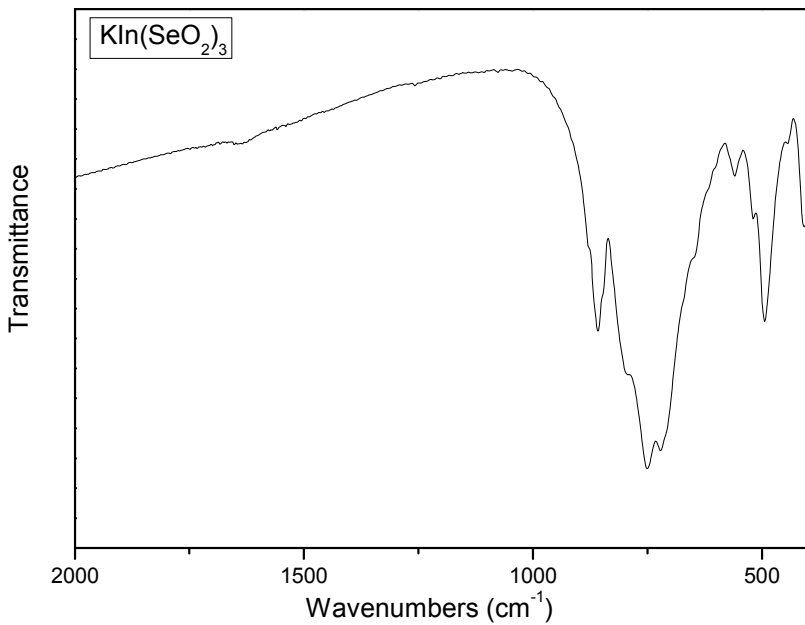
S8. Thermogravimetric analysis diagram for $\text{CsIn}(\text{SeO}_3)_2$



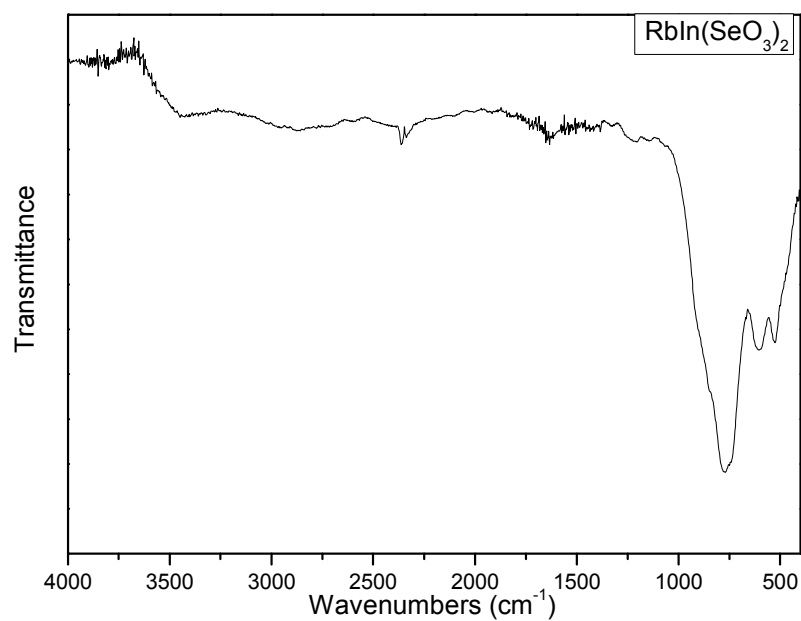
S9. IR spectrum for NaIn(SeO₃)₂



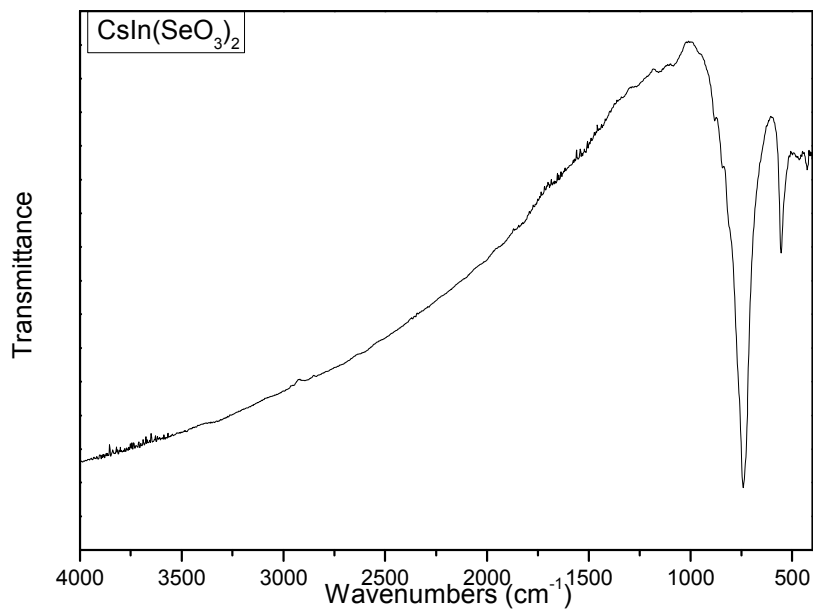
S10. IR spectrum for KIn(SeO₃)₂



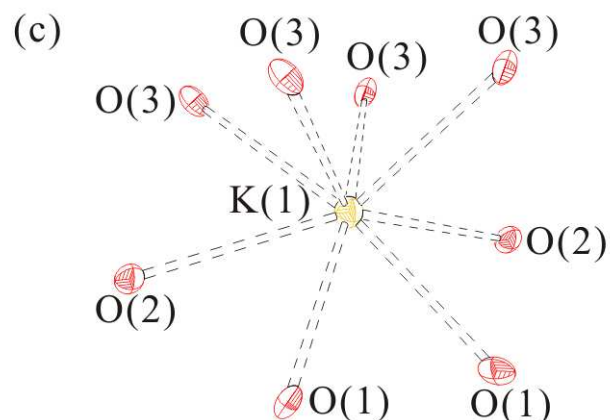
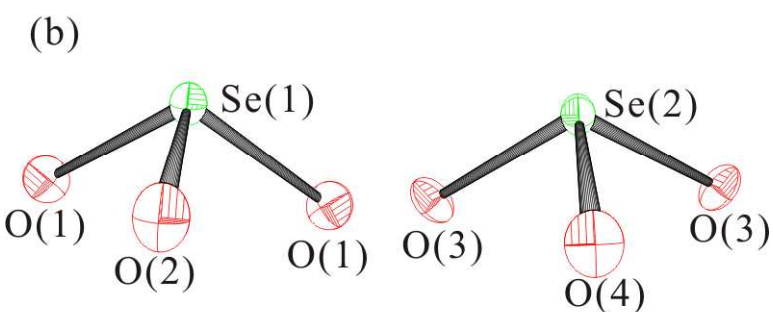
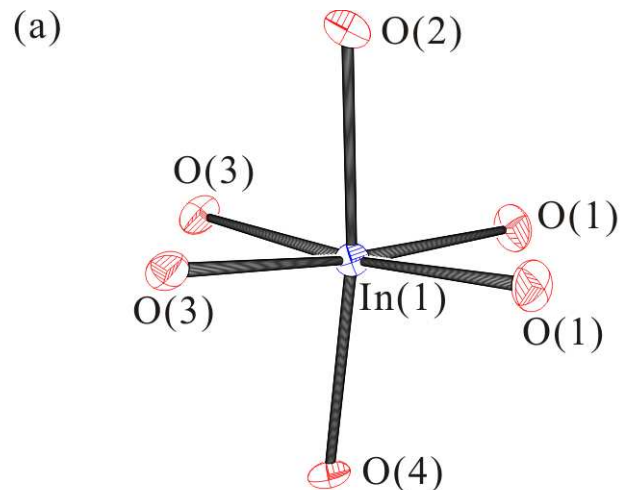
S11. IR spectrum for RbIn(SeO_3)₂



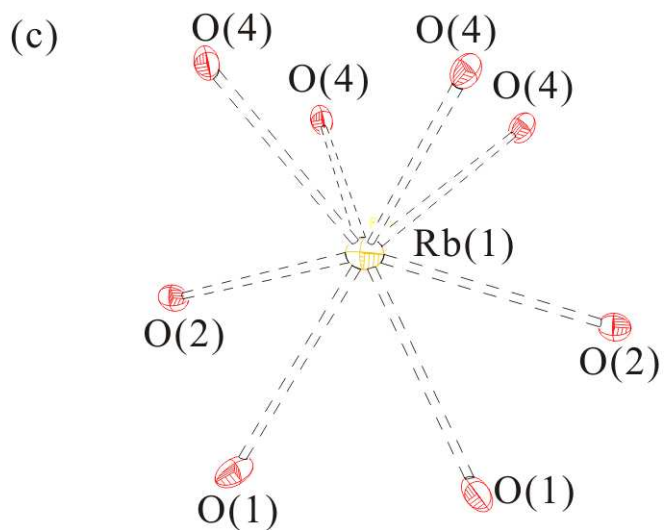
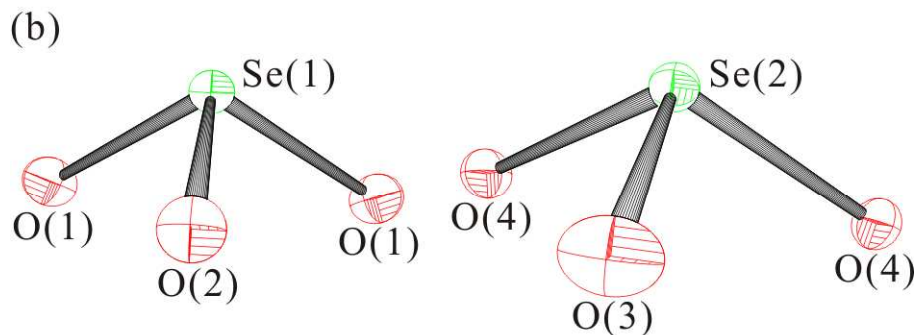
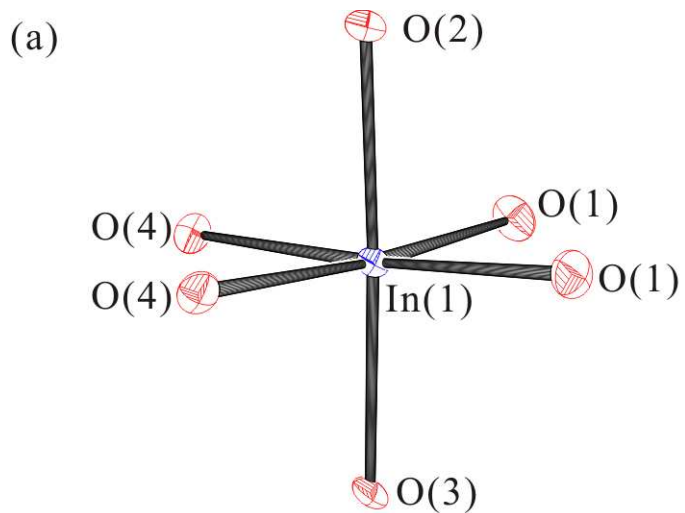
S12. IR spectrum for CsIn(SeO_3)₂



S13. ORTEP (50% probability ellipsoids) representations in $\text{KIn}(\text{SeO}_3)_2$ showing (a) the distorted InO_6 octahedron, (b) the asymmetric SeO_3 polyhedra, and (c) the KO_8 polyhedron.



S14. ORTEP (50% probability ellipsoids) representations in $\text{RbIn}(\text{SeO}_3)_2$ showing (a) the distorted InO_6 octahedron, (b) the asymmetric SeO_3 polyhedra, and (c) the RbO_8 polyhedron.



S15. ORTEP (50% probability ellipsoids) representations in $\text{CsIn}(\text{SeO}_3)_2$ exhibiting (a) the InO_6 octahedron, (b) the asymmetric SeO_3 polyhedra, and (c) the CsO_{12} hexagonal prism.

